






Article

Model based on an effective material removal rate to evaluate the specific energy consumption in grinding

A. Nápoles Alberro¹ , H.A. González Rojas¹ , A.J. Sánchez Egea^{2,*} , S. Hameed¹ , R.M. Peña Aguilar³ 

¹ Dept. of Mechanical Engineering (EPSEVG), Universidad Politécnica de Cataluña. Av. de Víctor Balaguer, 1, 08800 Vilanova i la Geltrú, Barcelona, Spain; amelia.napoles@upc.edu; hernan.gonzalez@upc.edu; hameeds@tcd.ie

² Dept. of Mechanical Engineering (EEBE). Universidad Politécnica de Cataluña. Av. Eduard Maristany, 16, 08019 Barcelona, Spain; antonio.egea@upc.edu

³ Dept. of Fluid Mechanics (EEBE). Universidad Politécnica de Cataluña. Av. Eduard Maristany, 16, 08019 Barcelona, Spain; reyna.mercedes.pena@iqs.url.edu

* Correspondence: antonio.egea@upc.edu

Abstract: The energy efficiency of grinding depends on the appropriate selection of cutting conditions, grinding wheel and workpiece material. Additionally, the estimation of specific energy consumption is a good indicator to control the energy consumed during the grinding process. Consequently, this study develops a model of material removal rate to estimate the specific energy consumption based on the measurement of active power consumed in a plane surface grinding of C45K with different thermal treatments and AISI 304. This model identifies and evaluates the power dissipated by sliding, ploughing and chip formation in a industrial-scale grinding process. Furthermore, the instantaneous positions of the abrasive grains during cutting are described to study the material removal rate. The estimation of specific chip formation energy is similar to that described by other authors in laboratory scale, which allows to validate the model and experiments. Finally, the results show that the energy consumed by sliding is the main phenomenon of energy dissipation in industrial-scale grinding process, where it is denoted that sliding energy by volume unity decreases as the depth of cut and speed of workpiece increase.

Keywords: Power consumption; Material removal rate; Specific energy consumption; Grain density; Modeling.

Nomenclature

e	Undeformed chip thickness
θ	Angular position
θ^*	Dimensionless angular position
k	Constant of proportionality
p	Depth of cut
G	Grain density
l_c	Contact length between wheel and workpiece
R_g	Grain's radius
d_g	Grain's diameter
l_g	Distance between grain
b_g	Width of grain during cutting
N_g	Number of grains
V_W	Speed of workpiece
V_S	Speed of grinding wheel
a_g	Feed rate
D_M	Diameter of the grinding wheel
R_M	Radius of the grinding wheel
A_{cg}	Section cut by a grain
MRR	Material removal rate
P	Total power consumption
P_{pl}	Power consumption by ploughing
P_{sl}	Power consumption by sliding
P_{ch}	Power consumption by chip formation
P_v	Idle power consumption
SCE	Specific cutting energy
SEC	Specific energy consumption
SEC_{sl}	Specific energy consumed by sliding
SEC_{ch}	Specific energy consumed by chip formation
SEC_{pl}	Specific energy consumed by ploughing

1. Introduction

The efficiency in machining processes acquires more attention due to high cost of energy, in which manufacturing cost represents a significant proportion of the total cost of final product [1]. The Industry 4.0 philosophy presents a global vision of virtualization for manufacturing of high quality parts [2,3]. These models and simulations help to optimize the conditions to execute the work cycle and desired results in manufacturing parts [4,5]. Hence, it is deduced that both the energy efficiency and virtualization require a model to analyze the behavior of the different manufacturing processes with respect to the operating conditions.

The models of specific energy are divided into two main groups: the models which evaluate the specific cutting energy SCE and the models which calculate the specific energy consumption SEC . The first group is based on experimental measurements of cutting forces during machining by using piezoelectric dynamometer located on the table of the grinding machine [6] or in the spindle where the grinding wheel is attached [7]. In this case, the recorded values of forces are multiplied with the peripheral speed of the grinding wheel to define the cutting power consumption. Other authors estimated the SCE by developing a function which related the active power of motor with the mechanical power developed by spindle during turning [8]. The same strategy was also used by González et al. [9] in drilling to investigate the influence of different cutting conditions.

However, the second group evaluated the SEC during the process by measuring the active power of motor, as it was done by Díaz et al. [10] during milling or Sánchez Egea et al. [11] during turning operations. Moreover, there are two ways to obtain material removal rate MRR . The first one is defined as the product of cutting cross section and speed of workpiece. The other one is defined as the product of effective section of cutting grains and cutting speed of grinding wheel [12]. Generally, the

authors used the first model, in which they considered the cutting section by the depth of cut and width of grinded zone [13]. Conversely, in the second model, the authors considered the effective cross section of cutting chip and number of grains corresponding to the contact area [14]. To make the second model applicable, the researchers used an equation for the maximum thickness of undeformed chip [15]. Based on the geometrical characteristics of chip formation, this thickness is defined as a function of cutting speed, speed of workpiece, depth of cut and the diameter of grinding wheel. This equation also included the normalized density of static grains G and a constant which indicated the average geometry of grain. There are cases in which G is defined as a function of angle of attack of grain [16]. Normally, authors calculated the chip thickness by using empirical data of G [17]. Due to the complexity of cutting edges of grinding wheel, it is well known that the G significantly influenced the grinding behaviour. Therefore, several authors measured the topography of grinding wheel through electron microscope [18]. So far, the models of SEC are characterized by macro level during iteration between workpiece and grinding wheel to predict the average value of chip thickness. A recent work developed the model of normal and tangential forces by considering the micro interaction between the workpiece and grinding tool [19].

In the present work, the SEC is obtained by measuring the active power consumed by motor which drives the grinding wheel. A model is developed to calculate the MRR under different cutting configurations and taking into account the interaction between grains and workpiece. The active power consumption is measured by a power analyzer connected to the three-phase electric motor. An equation of deformed chip thickness and effective cutting section is also proposed to accurately define the MRR . Finally, the chip thickness equation is defined as a function of radial position of each grain, cutting parameters and actual grain density of grinding wheel. Additionally, a laser distance sensor is used to measure the topography of the abrasive wheel and, ultimately, to calculate the grain density.

2. Model of specific energy consumption

In grinding, three phenomena occurred between the grinding wheel and workpiece. Firstly, the friction between the wheel and workpiece characterized by negligible small MRR . When the force of grains increased on the workpiece, an elastic and plastic deformation occurred, which produced a scratch with crests on the sides. The material was removed by increasing the force to produce chip formation [19]. In this work, it was considered that the power consumed in the grinding is due to the power dissipated by different phenomena involved in the process. These phenomena were: the friction between the wheel and workpiece (sliding), the plastic deformation without breakage (ploughing), and chip removal by shearing (chip formation) [20]. The power consumed by sliding, ploughing and chip formation mechanisms are P_{sl} , P_{pl} and P_{ch} , respectively. Then the total power consumed P during the process is equal to the sum of power consumed by each of above mentioned phenomena.

$$P = P_{sl} + P_{pl} + P_{ch} \quad (1)$$

In chip removal process, the SEC is directly proportional to the relation between the power consumed and MRR [21]. If equation (1) is divided by MRR and reorganized then equation (2) is obtained as follows:

$$\frac{P - P_{sl}}{MRR} = \frac{P_{pl}}{MRR} + SEC_{ch} \quad (2)$$

where SEC_{ch} is the specific energy consumed by chip formation.

During grinding, two types of cutting operations were defined due to the alternative movement of the table on which the workpiece was placed. If the movement was in the opposite direction to the peripheral speed V_s of grinding wheel, then this operation is called up-grinding. If the movement was in the same direction as V_s of wheel, then the operation is called down-grinding. In this work,

the grinding was conceived in the following way: the depth of cut was applied to workpiece when it started its movement in up-grinding. This step should not be repeated until down-grinding was completed. Therefore, during the movement of up-grinding, the sliding, ploughing and chip formation existed simultaneously. On the other hand, during down-grinding only sliding existed.

If the power consumed during up-grinding and power consumed during down-grinding are known, then the phenomena of ploughing and chip formation can be isolated. Hence, the difference between power consumed in up and down grinding was due to ploughing and chip formation, which were the phenomena that characterized cutting [22]. In this study, the power of two trajectories was measured by a power analyzer during grinding in dry condition with different cutting conditions and metallic alloys. The power consumed by motor was also measured during idle condition, i.e. when the wheel was not in contact with workpiece. Therefore, the active power consumption can be calculated by subtracting the power measured without cutting (idle) from the power in up and down grinding.

2.1. Model of an effective material removal rate in grinding

In grinding, it is difficult to define the geometry of cutting tool as the grinding wheel has different cutting grains distributed irregularly on the working surface and at the same time the grains have different cutting edges. The *MRR* is obtained by considering the geometric intersections between the grinding wheel and workpiece, as well as multiple grains involved in cutting. To define the model of *MRR*, firstly the equation of chip thickness and the section cut by a grain A_{cg} were obtained. Subsequently, the *MRR* by all cutting grains is calculated simultaneously. Figure 1 represents the section of material removed during up-grinding. It defined the radius of grinding wheel R_M , the angular position of grain θ , the contact length between grinding wheel and workpiece l_c and the cutting parameters such as speed of grinding wheel V_s , speed of workpiece V_w and depth of cut p . The undeformed chip thickness e was measured in the plane XY , and the A_{cg} was evaluated in the plane ZY which is perpendicular to the plane of grinding wheel and is represented by the section A-A.

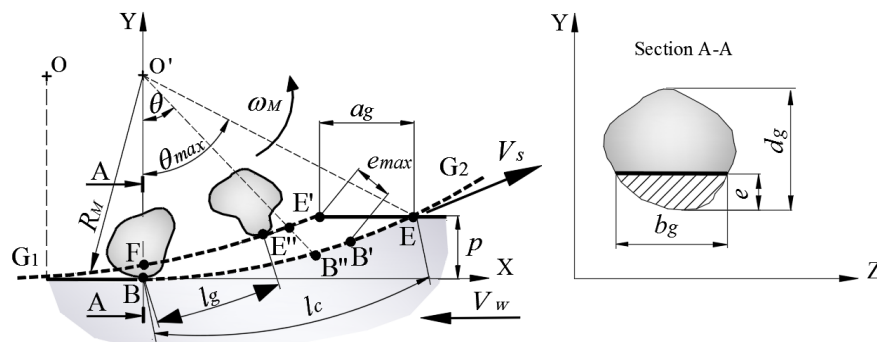


Figure 1. Characteristics of interaction between the grinding wheel and workpiece.

In this section, the evolution of chip thickness as a function of angular position of grain θ was analyzed. To define the chip thickness, it was assumed that the grains of grinding wheel were equally spaced like the teeth of milling cutter. Accordingly, Figure 1 shows the trajectories G_1 and G_2 of two abrasive grains that cut consecutively. The trajectory G_2 has a center displaced a distance OO' equivalent to the feed rate a_g which depends on the distance between the grains l_g and the speeds of workpiece V_w and the grinding wheel V_s . The zone of interest was defined by the points $BEE'F$, where l_g between grinding wheel and workpiece was defined by the arc BE and maximum thickness by the points $E'B'$. To obtain the coordinates of intersection of line $E''B''$ with curves G_1 and G_2 , the equations were developed to define the circumferential arcs of G_1 and G_2 and the line $O'B''$. Then, point E'' is defined by the intersection of the curve G_1 and line $O'E''$ as a function of θ . Therefore, the equations can be defined as a function of the dimensionless angular position θ^* defined as the ratio of

119 θ and θ_{max} .

120

$$\theta^* = \frac{\theta}{\sqrt{2 \cdot p / R_M}} \quad (3)$$

121 The chip thickness was defined as:

$$e = 2\theta^* \cdot \left(l_g \cdot \frac{V_W}{V_S} \right) \cdot \left(\frac{p}{D_M} \right)^{1/2} \quad (4)$$

122 where D_M is the diameter of the grinding wheel.

123

124 By considering the static density of grain constant, it was estimated that the distance between
125 grains is constant throughout the perimeter of grinding wheel. Then the length between grains l_g can
126 be deduced as:

$$l_g = \frac{1}{G \cdot b_g} \quad (5)$$

127 where b_g is the width of grain as a function of undeformed chip thickness e and diameter of grain d_g .

$$b_g = 2 \cdot \sqrt{d_g \cdot e} \quad (6)$$

128 Replacing (5) and (6) in (4) gave a useful expression for the e as follows:

$$e = \left(\frac{\theta^* \cdot V_W}{G \cdot V_S} \right)^{2/3} \cdot \left(\frac{p}{d_g \cdot D_M} \right)^{1/3} \quad (7)$$

129 The area of the material removed by grain A_{cg} corresponded to the effective section of cutting
130 by grain. To estimate A_{cg} , it was assumed that the geometric shape of grain can be approximated
131 to a sphere and only a part of grain cut the material [15]. For a sphere, the effective cutting area is a
132 function of e and the radius of grain R_g :

$$A_{cg} = \arccos(1 - e/R_g) \cdot R_g^2 - (R_g - e) \cdot R_g \cdot \sin(\arccos(1 - e/R_g)) \quad (8)$$

133 A_{cg} is different for each relative position of grain as the chip thickness e increases with the increase
134 of θ^* . The total area of cutting depends on the number of grains and will be equal to the sum of
135 instantaneous areas of each grain present along the contact length between the wheel and workpiece.
136 Finally, considering the number of grains N_g cut in the grinding width, the MRR by all grains in plane
137 ZY will be calculated as:

$$MRR = \sum_{i=1}^{N_g} (\overrightarrow{A_{cg}}(e_i) \times \overrightarrow{V_S}) \quad (9)$$

138 3. Experimental setup

139 In this work, two types of experiments were performed. The topography of the grinding wheel
140 was evaluated and the power consumed by motor was measured during grinding test. Two types
141 of metallic alloys were selected: ductile and brittle. This will be helped to understand the effect of
142 hardness of the material and the cutting parameters on the SEC .

143 3.1. Estimation of grain density in grinding wheel

144 The distance between two adjacent grains depends on the structure of grinding wheel. In grinding
145 tests, the grinding wheel of aluminium oxide A36H5V was used, which has 250 mm outside diameter,

76 mm mounting hole, 40 mm width and the grain size of number 36 according to manufacturer's certificate. According to FEPA standard [23], the characteristics of this grinding wheel are: $d_g=0.337$ mm and $l_g=0.67$ mm. The topography of wheel was measured to confirm the information provided by the manufacturer. The wheel was mounted on a divider head located on the table of a vertical milling machine. The measurements were made by using a laser (LDS-Laser distance sensor, model: LDS90/40, Canada) located on the spindle of the machine. The surface roughness was measured with an accuracy of 0.001 mm according to the data acquisition equipment (HBM, model: Spider-8, Germany). In total, eight profiles of surface roughness with an evaluation length of 5 mm each were measured across the width of the grinding wheel. For statistical analysis, the average value of length between grains was calculated. The Anderson Darling test was applied to the specimen and a probability of 0.570 was found. Consequently, it can be assumed that its distribution has a normal behaviour, as p-value was greater than 0.05. Figure 2a shows the surface roughness profile of grinding wheel in which the distance between grains was identified. The average grain density can be calculated by evaluating the number of peaks in the specimen. The average distance between grains was 0.775 mm with a confidence interval of 0.650-0.900 mm and the averaged G was 3.05 grains/mm² with a confidence interval of 3.030-3.676 grains/mm². The value of distance between grains was greater than the theoretical value indicated by the manufacturer and, therefore, the G was slightly smaller. On the other hand, diamond testings were performed with a maximum depth of cut of 0.02 mm and detached grains were collected for analysis. The main length of grains was measured by using optical magnifiers (Leica, model: M165C, Germany) shown in Figure 2b. Then, the equivalent diameter was calculated by assuming the grain geometry as a sphere. The Anderson Darling test was applied to the diameters and a p-value of 0.65 was obtained. Consequently, it can be assumed that the equivalent diameter has a normal behaviour with an average value of 0.347 mm and confidence interval of 0.300-0.394 mm.

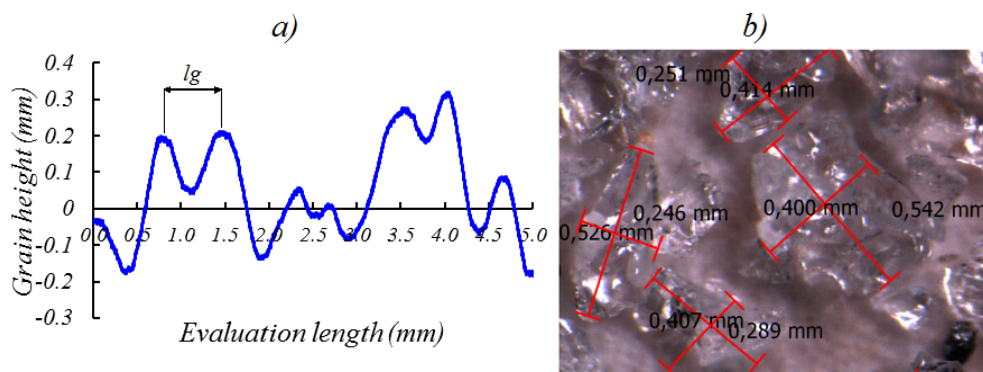


Figure 2. Characteristics of the grinding wheel A36H5V: a) the surface roughness profile and b) size of the detached grains.

3.2. Measurement of power consumption

The plane dry grinding experiments were carried out in a grinding machine (KAIR, model: T650, Germany) with a nominal power of 2.24 kW and rotation speed of grinding wheel of 1750 min⁻¹. Five grinding passes were made for each test specimen with dimensions of 30x10x130 mm. The material hardness was measured with a durometer (Wolpert, model: Testor HT, Germany). Table 1 shows average error dispersion with an interval of 95% confidence the material hardness of each metallic alloy. In total, five hardness values were recorded for each alloy, then an Anderson Darling test was applied to verify a normal distribution. The confidence interval was estimated by using a t-student test in the material's hardness measurements.

Table 1. Material hardness of metallic alloys.

Hardness Material (HRC)	C45K	C45K quenching	C45K tempering	AISI 304
	17.35 ± 1.38	56.16 ± 0.52	25.72 ± 0.72	19.85 ± 0.68

To evaluate the power consumption, the active power of an electric motor was recorded in three conditions: idle, up-grinding and down-grinding. The power was measured by an energy analyzer (HBM, model: Genesis eDrive Testing, Germany), where the current intensity, the voltage and the power consumed by the motor were recorded [24]. Since, the grinding machine was a three-phase machine, the wattmeter recorded the measurements of three phases. Then, these measurements were saved on files in ASCII format to be post-processed. These results allowed to identify the tie periods and power consumption during cutting in up and down-grinding and idle condition. Figure 3 shows the signals of power consumed while grinding C45K steel with a depth of cut of 0.020 mm and a speed of workpiece of 101 mm/s. In this figure, the path of up and down grinding and idle condition were identified with the average active power consumption of 259 W, 240 W and 54 W, respectively.

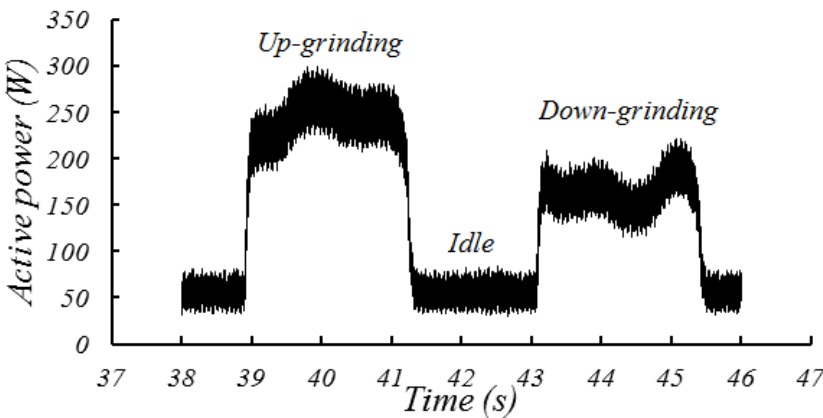


Figure 3. Signal of active power consumption by the electric motor.

4. Results and discussion

In equation (2), if the terms P , P_{sl} and MRR are known, then it is possible to find P_{pl} and SEC_{ch} by performing regression. These regression curves are estimated from experimental data performed with different cutting conditions, such as: depths of cut of 0.010 mm, 0.015 mm and 0.020 mm; the average speeds of workpiece of 57 mm/s, 101 mm/s and 150 mm/s and a constant rotation speed of grinding wheel of 1750 min⁻¹. These cutting conditions are similar to those frequently used by other authors [25]. Figure 4 shows the regression curves of each material from experimental data. In equation (2), the specific energy consumed during grinding SEC is defined as the ratio between P and MRR . While, the specific consumed in sliding SEC_{sl} is the ratio between the P_{sl} and MRR .

The regression applied to the experimental data of the materials C45K, C45K quenching, C45K tempering and AISI 304, have adjustment quality R^2 of 0.82, 0.84, 0.76 and 0.8, respectively. Figure 4 exhibits that when MRR increases, the SEC decreases gradually. From the graph, it is also noted that if MRR is very small then the SEC is higher, which is defined as a size effect [15]. The quality of the adjustment allows to validate the hypothesis that the SEC has asymptotic behaviour defined by the equation (2). This behaviour is similar to the model developed by Diaz et al. [10] and by Zhong et al. [26] for milling and turning operations, respectively. Moreover, Table 2 exhibits the results of SEC associated with the phenomenon involved in grinding, SEC_{sl} , SEC_{pl} and SEC_{ch} . Where specific energy consumed by ploughing SEC_{pl} is the ratio between P_{pl} and MRR . The average energy consumed by sliding SEC_{sl} is 92%, 85%, 57% and 94% of the total energy consumed by C45K, C45K

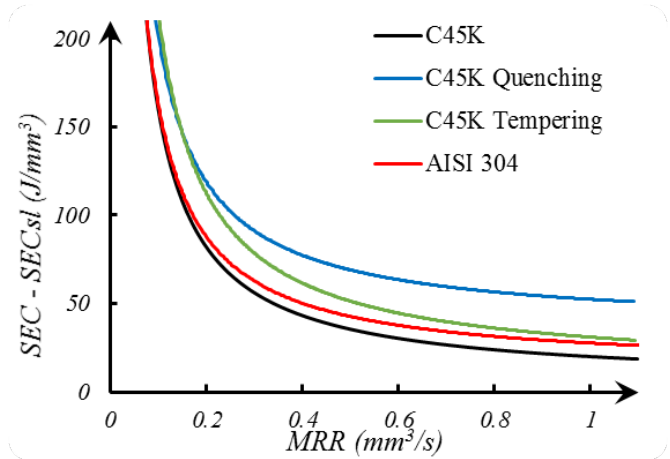


Figure 4. Specific energy consumption versus the material removal rate.

quenching, C45K tempering and AISI 304, respectively. This work characterizes the industrial-scale grinding process, where SEC_{sl} is an order of magnitude greater than SEC_{ch} . Also, as compared to other authors who studied grinding at the laboratory scale by using a single grain grinding wheel [6,25], which found small values of SEC_{sl} . In addition, the SEC_{ch} values for C45K steel and C45K quenching reported in this work are similar in magnitude to the SEC_{ch} values reported by Marinescu et al. [27]. Furthermore, SEC_{sl} , SEC_{pl} and SEC_{ch} of C45K quenching steel presents greater values than the other metallic alloys. This is due to the fact that the greater the material hardness of workpiece, the higher will be SEC required for chip cutting [10].

Table 2. Average specific energy consumption of different indices in plane dry grinding.

Metallic alloy	SEC (J/mm ³)	SEC_{sl} (J/mm ³)	SEC_{pl} (J/mm ³)	SEC_{ch} (J/mm ³)
C45K	655	602	30	8
C45K quenching	1805	1541	132	36
C45K tempering	351	201	113	11
AISI 304	958	901	36	13

Figure 5a shows the results of SEC_{sl} for different depths of cut, types of alloys and the thermal treatments. It is shown that the greater the depth of cut, the lower will be the contribution of SEC_{sl} , which is similar to the behaviour reported by Ghosh et al. [28]. This is due to the presence of a large number of cutting grains and, subsequently, the area subjected to friction is smaller [12]. Figure 5b exhibits the results of SEC_{sl} for an average depth of 0.015 mm at different speeds of workpiece and different materials. In general, SEC_{sl} decreases as speed of workpiece increases. A similar behaviour was reported by Bakkal et al. [21], which described that in grinding the ratio between the tangential and normal forces increased as the speed of workpiece increased.

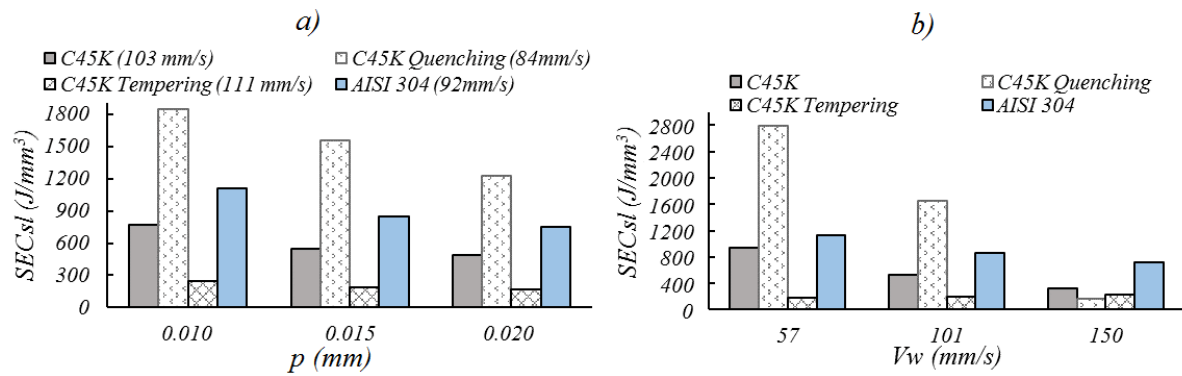


Figure 5. Relationship between the specific energy consumption versus a) the depth of cut and b) the speed of workpiece.

The results show that high energy consumption is found for lower depths of cut and speeds of workpiece, except C45K tempering material which shows constant values of energy consumption when these two operational parameters are increased. In particular, quenching requires more energy for low and medium speeds of workpiece and depths of cut, whereas tempering presents similar low values of energy consumption for higher depths of cut and speeds of workpiece. It can be due to the differences in hardness at the surface of materials and their elastoplastic behavior. Finally, both materials C45K and AISI 304 exhibit the same trend of decreasing the energy consumption by increasing the depth of cut and the speed of workpiece. Thus, thermal treatments have a noticeably influence on the energy consumption, but also the temperature in grinding is crucial and depends on the selection of the operational parameters [29]. In summary, the model of MRR develops in the present study is different from other models, as the thickness of the chip (7) and the section of cutting grain (8) are the function of the angular position of the grain. This is different from Zhenzhen et al. [16], who considered the maximum value of chip thickness to estimate MRR . On the other hand, chip thickness (7) has the same variables and structure as defined by Malkin et al. [15]. The only difference is in the exponent which affects the G and speeds of grinding wheel and workpiece. Other models calculated the MRR as a product of depth of cut, grinding width and speed of workpiece [30]. This last model did not incorporate the speed of grinding wheel in the definition of MRR , as compared to the model presented in this work.

5. Conclusions

The present paper proposed a model to calculate the MRR and specific energy consumption in grinding, where the depth of cut, speed of workpiece, the effective cutting section, grain density and material hardness play a crucial role. Accordingly, the main conclusions can be summarized as follow:

- A model has been successfully developed to evaluate the energy dissipated by sliding, ploughing and chip formation phenomena in an industrial-scale grinding process. In general, the sliding energy governs the process of energy dissipation in grinding.
- The energy dissipated by sliding phenomenon decreases when the depth of cut and speed of workpiece increase, allowing to reduce the energy consumption and manufacturing cost during grinding.
- The model also allows to find the specific energy consumed by chip formation, which is the limit value defined by the asymptotic behaviour experienced by the SEC . This validates the hypothesis that during down-grinding, the energy calculated by the analyzer corresponds to the energy dissipated by sliding.

The future work will be focused on optimize the grinding process by reducing the energy consumption during the process. For this, it is necessary to use a wider range of operational parameters V_W and p to investigate the behavior of the SEC and its local minimum.

Acknowledgments: The authors likewise acknowledges the funding from Serra Húnter programme (Generalitat de Catalunya, ref. UPC-LE-304) and Universidad Politécnica de Cataluña. HBM Ibérica is acknowledged for let us use the device for measuring the power consumption in this work. Thanks also to Juan Alsina from HBM for the valuable support with the energy analyzer (Genesis eDrive Testing).

Author Contributions: Conceptualization: H.A.G.R. and A.N.A. Data curation: A.N.A., H.A.G.R and A.J.S.E. Formal analysis: H.A.G.R and A.J.S.E. and S.H. Funding acquisition: A.J.S.E. and H.A.G.R. Methodology: A.N.A., R.M.P.A. and H.A.G.R. and S.H. Software: A.J.S.E., R.M.P.A. and A.N.A. Supervision: H.A.G.R and A.J.S.E. Validation: H.A.G.R. and R.M.P.A. Writing original draft: A.N.A. and S.H. Writing, review and editing: H.A.G.R and A.J.S.E.

Conflicts of Interest: All the authors who sign this manuscript do not have any conflict of interest to declare. Furthermore, the corresponding author certifies that this work has not been submitted to or published in any other journal.

References

- Merchant M.E. An interpretive look at 20th century research on modeling of machining. *Machining Science and Technology*, **1998**, 2(2), 157-163. Doi: 10.1080/10940349808945666
- Zheng P. et al. Smart manufacturing systems for Industry 4.0: Conceptual framework, scenarios, and future perspectives. *Frontiers of Mechanical Engineering*, **2018**, 13(2), 137-150. DOI: 10.1007/s11465-018-0499-5
- Sánchez Egea A.J., López de Lacalle L.N.L. Máquinas, procesos, personas y datos, las claves para la revolución 4.0. *DYNA Ingeniería e Industria*, **2018**, 93(6), 576-577. DOI: 10.6036/8807
- Aurich J.C., Linke B., Hauschild M., Carrella M., Kirsch B. Sustainability of abrasive processes. *CIRP Ann. - Manuf. Technol.*, **2013**, 62(2), 653-672. DOI: 10.1016/j.cirp.2013.05.010
- Calleja A., Tabernero I., Fernández A., Celaya A., Lamikiz A., López de Lacalle L.N. Improvement of strategies and parameters for multi-axis laser cladding operations. *Optics and Lasers in Engineering*, **2014**, 56, 113-120. Doi: 10.1016/j.optlaseng.2013.12.017
- Azizi A., Mohamadyari M. Modeling and analysis of grinding forces based on the single grit scratch. *Int. J. Adv. Manuf. Technol.*, **2015**, 78(5-8), 1223-1231. DOI: 10.1007/s00170-014-6729-z
- Li L., J. Yan J., Xing Z. Energy requirements evaluation of milling machines based on thermal equilibrium and empirical modelling. *J. Clean. Prod.*, **2013**, 52, 113-121. DOI: 10.1016/j.jclepro.2013.02.039
- Hameed A., Rojas H.A.G., Benavides J.I.P., Alberro A.N., Egea A.J.S. Influence of the regime of electropulsing-assisted machining on the plastic deformation of the layer being cut. *Materials (Basel)*, **2018**, 11(6). DOI: 10.3390/ma11060886.
- González Rojas H.A., Nápoles Alberro A., Sánchez Egea A.J. Machinability estimation by drilling monitoring. *DYNA Ing. e Ind.*, **2018**, 93, 663-667. DOI: 10.6036/8821
- Diaz N., Redelsheimer E., Dornfeld D. Energy Consumption Characterization and Reduction Strategies for Milling Machine Tool Use. In: Hesselbach J., Herrmann C. (eds) *Glocalized Solut. Sustain. Manuf.* Springer, Berlin, Heidelberg, **2011**, 263-267. DOI: 10.1007/978-3-642-19692-8-46
- Sánchez Egea A.J., González Rojas H.A., Montilla Montaña C.A., Kallewaard Echeverri V. Effect of electroplastic cutting on the manufacturing process and surface properties. *Journal of Materials Processing Technology*, **2015**, 222, 327-334. DOI: 10.1016/j.jmatprotec.2015.03.018
- Hecker R.L., Liang S.Y., Wu X.J., Xia P., Jin D.G.W. Grinding force and power modeling based on chip thickness analysis. *Int. J. Adv. Manuf. Technol.*, **2007**, 33(5-6), 449-459. DOI: 10.1007/s00170-006-0473-y
- Anderson D., Warkentin A., Bauer R. Experimental validation of numerical thermal models for dry grinding. *J. Mater. Process. Technol.*, **2008**, 204(1-3), 269-278. DOI: 10.1016/j.jmatprotec.2007.11.080
- Agarwal S., Rao P.V. Predictive modeling of force and power based on a new analytical undeformed chip thickness model in ceramic grinding. *Int. J. Mach. Tools Manuf.*, **2013**, 65, 68-78. DOI: 10.1016/j.jmachtools.2012.10.006
- Malkin S., Guo C. *Grinding Technology - Theory and Applications of Machining with Abrasives* (2nd Edition). Industrial Press, **2008**. ISBN: 9780831132477

16. Zhenzhen C., Jiuhua X., Wenfeng D., Changyu M. Grinding performance evaluation of porous composite-bonded CBN wheels for Inconel 718. *Chinese J. Aeronaut.*, **2014**, 27(4), 1022-1029. DOI: 10.1016/j.cja.2014.03.015
17. Lee Y.M., Jang S.G., Jang E.S. Grinding characteristics of polycrystalline silicon. *Rev. Adv. Mater. Sci.*, **2013**, 33(3), 287-290.
18. Nguyen A.T., Butler D.L. Correlation of grinding wheel topography and grinding performance: A study from a viewpoint of three-dimensional surface characterisation. *J. Mater. Process. Technol.*, **2008**, 208(1-3), 14-23. DOI: 10.1016/j.jmatprotec.2007.12.128
19. Rowe W.B. *Principles of Modern Grinding Technology*. Princ. Mod. Grind. Technol., **2014**. ISBN: 978-0-323-24271-4
20. Malkin S., Guo C. Thermal Analysis of Grinding. *CIRP Ann. - Manuf. Technol.*, **2007**, 56(2), 760-782. DOI: 10.1016/j.cirp.2007.10.005
21. Bakkal M., Serbest E., Karipcin I., Kuzu A.T., Karagüzel U., Derin B. An experimental study on grinding of Zr-based bulk metallic glass. *Adv. Manuf.*, **2015**, 3(4), 282-291. DOI: 10.1007/s40436-015-0121-6
22. Kumar V., Salonitis K., Empirical estimation of grinding specific forces and energy based on a modified Werner grinding model. *Procedia CIRP*, **2013**, 8, 287-292. DOI: 10.1016/j.procir.2013.06.104
23. FEPA - Grains Standards Federation of the European Producers of Abrasives. ISO/TC 29/SC 5. Grinding wheels and abrasives **2006**.
24. Gontarz A.M., Weiss L., Wegener K. Energy Consumption Measurement with a Multichannel Measurement System on a machine tool. *Proc. Int. Conf. Innov. Technol.*, **2010**, 499-502. DOI: 10.3929/ethz-a-007577653
25. Singh V., Venkateswara Rao P., Ghosh S. Development of specific grinding energy model. *Int. J. Mach. Tools Manuf.*, **2012**, 60, 1-13. DOI: 10.1016/j.ijmachtools.2011.11.003
26. Zhong Q., Tang R., Lv J., Jia S., Jin M. Evaluation on models of calculating energy consumption in metal cutting processes: a case of external turning process. *Int. J. Adv. Manuf. Technol*, **2015**, 82(9-12), 2087-2099. DOI: 10.1007/s00170-015-7477-4
27. Marinescu I., M. Hitchiner M., E. Uhlmann E., Brian Rowe W. *Handbook of Machining with Grinding Wheels*, Edition: 1st Publisher: crc press, **2007**. ISBN: 978-1-57444-671-5
28. Ghosh S., Chattopadhyay A.B., Paul S. Modelling of specific energy requirement during high-efficiency deep grinding. *International Journal of Machine Tools and Manufacture*, **2008**, 48(11), 1242-1253. DOI: 10.1016/j.ijmachtools.2008.03.008
29. Urgoiti L., Barrenetxea D., Sánchez J.A., Pombo I., Álvarez J. On the Influence of Infra-Red Sensor in the Accurate Estimation of Grinding Temperatures. *Sensors*, **2018**, 18(4134), 1-10. DOI: 10.3390/s18124134
30. Hacksteiner M., Peherstorfer H., Bleicher F. Energy efficiency of state-of-the-art grinding processes. *Procedia Manufacturing*, **2018**, 21, 717-724. DOI: 10.1016/j.promfg.2018.02.176